# Raman Studies on the Interaction of the Reactants with the Platinum Nanoparticle Surface during the Nanocatalyzed Electron Transfer Reaction

**Radha Narayanan and Mostafa A. El-Sayed***

*Laser Dynamics Laboratory, School of Chemistry and Biochemistry, Georgia Institute of Technology, Atlanta, Georgia 30332-0400*

*Received: June 28, 2005; In Final Form: August 9, 2005*

Raman studies are conducted to understand the specific interactions between the individual reactants and the platinum nanoparticle surface during the nanocatalyzed electron transfer reaction between hexacyanoferrate (III) ions and thiosulfate ions. When Pt nanoparticles are added to the thiosulfate ion solution, a shift in the symmetric SS stretching mode is observed compared to the frequency observed for the free thiosulfate ions in solution, suggesting that binding to the Pt nanoparticle surface occurs via the $S^-$ ion. It is also observed that there are no shifts in the symmetric and asymmetric OSO bending or SO stretching frequencies. This suggests that the thiosulfate ions do not bind to the nanoparticle surface via the $O^-$ ion. When platinum nanoparticles are added to the hexacyanoferrate(III) ion solution, evidence is found for both adsorbed hexacyanoferrate(III) ions and a platinum cyanide complex. For adsorbed hexacyanoferrate(III) ions, the CN stretching frequency is observed at 2101 $cm^{-1}$ and the Fe−C stretching frequency is found at 368 $cm^{-1}$. The observed CN stretching frequencies located at 2147 and 2167 $cm^{-1}$ provide strong evidence that there is a $Pt(CN)_4^{2-}$ platinum cyanide complex formed. In addition, the Pt−C≡N band is also observed at 2054 $cm^{-1}$. These observed bands provide spectroscopic evidence that the hexacyanoferrate(III) ions dissolve by forming a complex with the surface platinum atoms of the nanoparticles. Raman spectra of the product mixtures are obtained after the completion of the reaction when carried out with higher reactant concentrations to observe the Raman spectra, but with a similar 10:1 ratio of thiosulfate to hexacyanoferrate(III) ions as used previously, with and without PVP−Pt nanoparticles at a correspondingly higher concentration. It is observed that there are no shifts in the characteristic Raman bands associated with hexacyanoferrate(II) ions and no evidence for the formation of adsorbed hexacyanoferrate(II) species or platinum cyanide complexes in the presence of the platinum nanoparticles. In addition, there is evidence for the shifted symmetric SS stretching mode, suggesting that some of the unreacted thiosulfate (present in large excess) is bound to the Pt nanoparticle surface. Thus, under the actual reaction conditions, the hexacyanoferrate(III) ions preferentially react with adsorbed thiosulfate ions to form the reaction products, and this supports the surface catalytic mechanism we proposed previously.

## Introduction

Since nanoparticles have a large surface:volume ratio, they are attractive as catalysts compared to bulk catalytic materials. The study of colloidal nanocatalysts has been very active recently and has been described in many review articles.[1−8] It is worth noting that there have been only a few studies in which colloidal metal nanoparticles have been characterized before and after their catalytic function.[9−13] We have previously conducted detailed studies on the effect of the catalytic process on the size and shape of platinum and palladium nanoparticles used as catalysts.[14−20] In many of these studies, we also analyzed the effect of the individual reactants on the nanoparticle size and shape, and these studies have provided clues about the gross surface catalytic mechanism of the reaction.

One reaction that we studied is the Suzuki reaction between phenylboronic acid and iodobenzene catalyzed by spherical polyvinylpyrrolidone (PVP)-capped Pd nanoparticles,[18] spherical polyamidoamine-OH (PAMAM-OH) Generation 4 stabilized Pd nanoparticles,[19] and tetrahedral PVP-capped Pt nanoparticles.[20] We conducted studies on the effect of the individual reactants on the size of spherical PVP-capped Pd nanoparticles and spherical PAMAM-OH Generation 4 encapsulated Pd nanoparticles. In both cases, we observed that when the nanoparticles are refluxed in the presence of phenylboronic acid, the Ostwald ripening process was inhibited, while the growth process continued to occur in the presence of iodobenzene.[18,19] In the case of tetrahedral PVP-capped Pt nanoparticles, we observed that when the nanoparticles are refluxed in the presence of phenylboronic acid, the nanoparticles maintained their tetrahedral shape, while they transformed to the spherical shape in the presence of iodobenzene.[20] In all three cases, it was proposed that the mechanism of the Suzuki reaction involves the phenylboronic acid binding to the nanoparticle surface and reacting with iodobenzene present in solution. We also conducted Fourier transform infrared spectroscopy (FTIR) studies in an effort to understand the mode of binding of phenylboronic acid to the nanoparticle surface.[21] From these studies, we showed that the phenylboronate anion binds to the Pd nanoparticle surface via the B−O−Pd bond in a bridged fashion and that iodobenzene does not bind to the nanoparticle surface. As a result, the FTIR studies confirm the surface catalytic mechanism of the Suzuki reaction that we proposed previously.[18−20]

Another reaction that we studied is the electron transfer reaction between hexacyanoferrate(III) ions and thiosulfate ions to form hexacyanoferrate(II) ions and tetrathionate ions. We

* To whom correspondence should be addressed. E-mail: mostafa.el-sayed@chemistry.gatech.edu.

10.1021/jp053526k CCC: $30.25 
Published on Web 09/10/2005

have used tetrahedral,[15−17] cubic,[15−17] and spherical[14−16] platinum nanoparticles to catalyze this reaction. We showed that during the early stages of the reaction, the catalytic activity was dependent on the nanoparticle shape.[15] However, during the course of the entire reaction, changes in the nanoparticle shape as well as corresponding changes in the activation energy took place.[16] In addition, the rate of shape change was faster for the tetrahedral nanoparticles than for the cubic nanoparticles.[17] In many of these studies, we also examined the effect of exposing the nanoparticles to individual reactants on the size and shape of the nanoparticles.[14,17] We observed that exposing the nanoparticles to hexacyanoferrate(III) ions resulted in a reduction in the size of the spherical platinum nanoparticles and dissolution of corner and edge atoms in the case of the tetrahedral platinum nanoparticles. We proposed that these changes could be due to the dissolution of surface platinum atoms to form a platinum complex via the $CN^-$ group present in the hexacyanoferrate(III) ions. When the nanoparticles were added to the thiosulfate ions, the size and shape of the platinum nanoparticles were maintained. This could be due to the thiosulfate ions binding to the nanoparticle surface and stabilizing it. On the basis of these observations, we proposed that the surface catalytic mechanism involved the thiosulfate ions binding to the nanoparticle surface and reacting with the hexacyanoferrate(III) ions present in solution.[14,17]

In the study presented here, we use Raman spectroscopy to understand the specific interactions of the individual reactants associated with the electron transfer reaction with the platinum nanoparticle surface. These studies will help determine the mode of binding of thiosulfate ions onto the nanoparticle surface as well as provide more details about how the hexacyanoferrate(III) ions interact with the platinum nanoparticle surface. We also use Raman spectroscopy to study the product mixture obtained after the reaction under similar reaction conditions, 10:1 ratio of thiosulfate to hexacyanoferrate(III) ions, with and without PVP−Pt nanoparticles at a correspondingly high concentration, to spectroscopically determine the exact surface catalytic mechanism that takes place.

## Experimental Section

**Synthesis of PVP−Pt Nanoparticles.** The PVP−Pt nanoparticles are synthesized as described previously[14] by the reduction of the platinum precursor salt, $K_2PtCl_4$, with ethanol. A solution containing 3 mL of 0.01 M $K_2PtCl_4$, 33 mL of doubly deionized water, 0.0667 g of PVP, and 4 drops of 1 M HCl is heated. When the solution begins to reflux, 14 mL of ethanol is added. The solution is then refluxed for 3 h, and a dark brown colloidal Pt solution is formed. A drop of the solution is spotted onto a Formvar-stabilized copper TEM grid, and a JEOL 100C transmission electron microscope (TEM) is used to characterize the size of the nanoparticles. For the solution-based Raman studies, it is necessary to have concentrated nanoparticle solutions. As a result, the nanoparticles are rotovaped to concentrate the nanoparticles down to a volume of 5 mL.

**Raman Studies.** For the studies on the interactions of the individual reactants on the Pt nanoparticle surface, aqueous solutions of 0.25 M hexacyanoferrate(III) ions and 0.25 M thiosulfate ions are prepared. Solutions of PVP−Pt nanoparticles with hexacyanoferrate(III) ions and solutions of PVP−Pt nanoparticles with thiosulfate ions are also prepared in water, and the reactant concentration is kept at 0.25 M in both cases. For the studies of the interactions of the reactants at the actual reaction condition ratio, solutions of hexacyanoferrate(III) ions with thiosulfate ions [10:1 ratio of thiosulfate to hexacyanoferrate(III) ions] in the presence and absence of PVP−Pt nanoparticles at a correspondingly high concentration are prepared. To observe the Raman spectra, we use concentrations that are 120 times higher than the concentrations used in our previous studies.[14−17] In the current study, we use 1 M thiosulfate, 0.1 M hexacyanoferrate(III) ions, and 17.7 $\mu$M Pt nanoparticles.

A few drops of each solution are placed onto the aluminum foil substrate for the Raman studies. In the case of the reaction mixtures, the Raman spectra of these solutions are recorded after the reaction is finished. The Raman spectra are obtained in the region from 3500 to 200 $cm^{-1}$ for these solutions using the Holoprobe Raman microscope by Kaiser Optical Systems. The laser excitation wavelength is at 785 nm. The background spectrum of aluminum foil is subtracted from each subsequent spectrum that is acquired. An acquisition time of 15 min is used to collect each spectrum in order to obtain a good signal-to-noise ratio. In addition, a cosmic ray filter is also used during the collection of the Raman spectra.

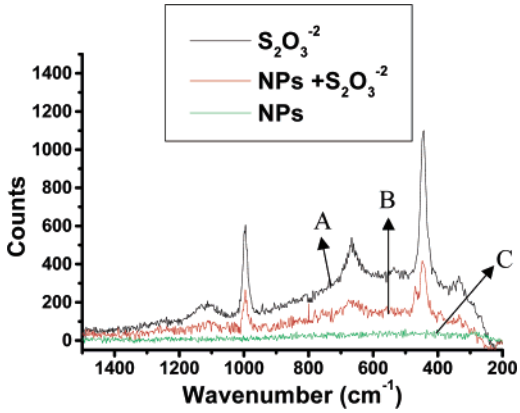


**Figure 1.** Raman spectra of solutions of thiosulfate ions (A), PVP−Pt nanoparticles with thiosulfate ions (B), and PVP−Pt nanoparticles (C) in the region of 1400−200 $cm^{-1}$.

**TABLE 1: List of Characteristic Raman Vibrational Modes Associated with Thiosulfate and Frequencies Observed for the Solution of Thiosulfate Ions by Themselves and for the Solution of Thiosulfate Ions Added to the PVP−Pt Nanoparticles**

| Raman vibrational mode | thiosulfate ($cm^{-1}$) | PVP−Pt nanoparticles + thiosulfate ($cm^{-1}$) |
|---|---|---|
| out-of-plane SSO bending[22] | 335 (m) | 339 (w) |
| symmetric SS stretching[22] | 444 (vs) | 448 (s), 470 (m, sh) |
| asymmetric OSO bending[22] | 536 (w) | 535 (vw) |
| symmetric OSO bending[22] | 667 (m) | 667 (w) |
| symmetric SO stretching[22] | 995 (vs) | 996 (s) |
| asymmetric SO stretching[22] | 1112 (w) | 1112 (vw) |

## Results and Discussion

**Raman Studies on Thiosulfate/Pt Nanoparticle Mixtures.** Figure 1 shows the Raman spectra acquired for solutions of PVP−Pt nanoparticles, thiosulfate ions, and PVP−Pt nanoparticles + thiosulfate ions in the region from 1400 to 200 $cm^{-1}$. The Raman spectra in the region from 3500 to 1400 $cm^{-1}$ are not shown since there are no spectral features present in this region for all three types of solutions. Table 1 summarizes the major characteristic Raman modes observed as well as their peak maximum values. The assignments of the Raman modes observed in thiosulfate ions are obtained from a previous study reported in the literature.[22] As can be seen in Figure 1, the PVP−Pt nanoparticles by themselves have only few very weak bands that do not interfere with the bands associated with thiosulfate ions.

**SCHEME 1: Schematic of the Chemical Structure of Thiosulfate Ions and Two Possible Binding Modes (via the S− ion or via the O− ion) When It Is Added to the Platinum Nanoparticles**

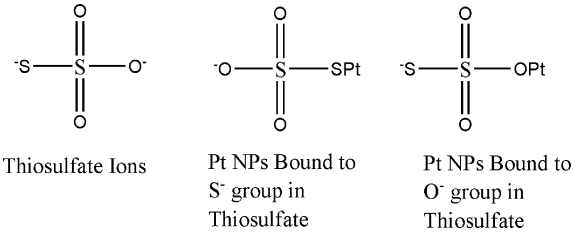


Scheme 1 shows the chemical structure of thiosulfate ions and the two possible binding modes that can occur when they are added to the Pt nanoparticles.

When Pt nanoparticles are added to the thiosulfate ion solution for 2 days, it is observed that there is a shift in the symmetric SS stretching frequency from 444 to 470 $cm^{-1}$. This shift suggests that the thiosulfate ions bind to the Pt nanoparticle surface via the $S^-$ ion. It is also worth noting that the unshifted SS stretching frequency also appears at 448 $cm^{-1}$, suggesting that there is also some free thiosulfate ions present in solution that are not bound to the Pt nanoparticle surface.

It is observed that there are no shifts in the symmetric and asymmetric OSO bending modes as well as the symmetric and asymmetric SO stretching modes associated with thiosulfate ions upon exposure to the Pt nanoparticles. This provides evidence that binding does not take place via the $O^-$ ion present in thiosulfate ions. As a result, the thiosulfate ions bind to the nanoparticle surface only through the $S^-$ ion. Previously,[14,17] we proposed that thiosulfate ions stabilize the nanoparticle surface since it can act as a capping agent by binding to the nanoparticle surface via the $S^-$ ion. The Raman studies conducted here provide spectroscopic evidence that the thiosulfate ions do indeed bind to the nanoparticle surface via the $S^-$ ion and confirm what we proposed previously.[14,17]

**Raman Studies on Hexacyanoferrate(III)/Pt Nanoparticle Mixtures.** Raman studies are also conducted to determine how the hexacyanoferrate(III) ions interact with the Pt nanoparticle surface. It is worth noting that we do not expect any enhancement of Raman bands to take place since the excitation wavelength of the laser is at 785 nm and this is far away from the surface plasmon band of platinum nanoparticles, which occurs in the UV region. As a result, the Raman bands that occur under these conditions are due to normal Raman scattering and not due to surface-enhanced Raman scattering. Figure 2 shows the Raman spectra obtained for hexacyanoferrate(III) ions, PVP−Pt nanoparticles + hexacyanoferrate(III) ions, and PVP−Pt nanoparticles in the region of 1400−200 $cm^{-1}$ (Figure 2a) and 2500−1800 $cm^{-1}$ (Figure 2b). The regions from 1800 to 1400 $cm^{-1}$ and from 3500 to 2500 $cm^{-1}$ are not shown since there are no peaks present in this region in all three cases. Again, it can be seen that the PVP−Pt nanoparticles by themselves have only few weak bands and these bands do not interfere with those associated with the hexacyanoferrate(III) ions.

The hexacyanoferrate(III) ions have four characteristic vibrational frequencies in the region from 1400 to 200 $cm^{-1}$. The Fe−CN stretching frequency is located[23] at 389 $cm^{-1}$ in the case of hexacyanoferrate(III) ions by themselves, and it is greatly diminished in magnitude and shifts to 368 $cm^{-1}$ upon exposure to the Pt nanoparticles. The shift in the frequency could be due to the adsorption of hexacyanoferrate(III) ions to the Pt nanoparticles. In the hexacyanoferrate(III) ions by themselves, there are three Fe−C stretching modes.[24,25] The $(Fe-C)_{br}$ stretching mode occurs at 490 $cm^{-1}$, the $(Fe-C)_{rad}$ stretching mode occurs at 540 $cm^{-1}$, and the $(Fe-C)_{ax}$ stretching mode occurs at 593 $cm^{-1}$. All three of these Fe−C stretching modes do not shift when the hexacyanoferrate(III) ions are added to the Pt nanoparticles, and there is enhancement in these peaks. This suggests that there are free hexacyanoferrate(III) ions present in solution.

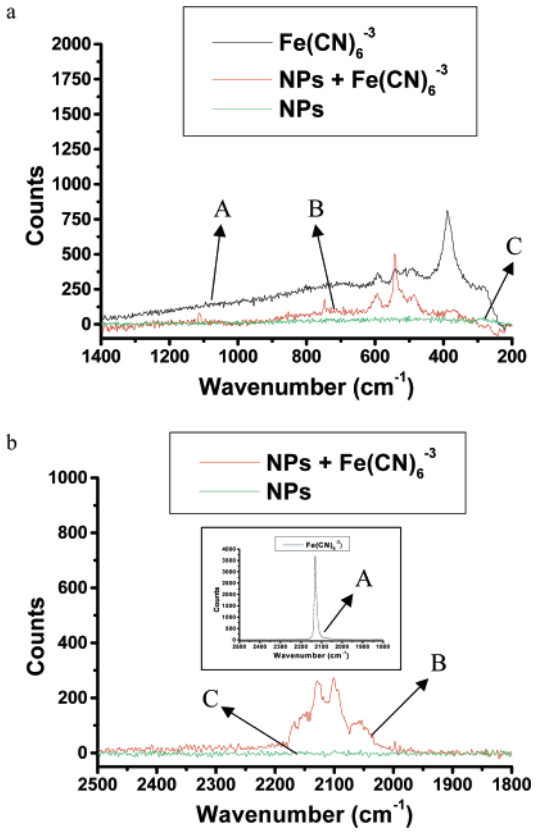


**Figure 2.** Raman spectra of solutions of hexacyanoferrate(III) ions (A), PVP−Pt nanoparticles with hexacyanoferrate(III) ions (B), and PVP−Pt nanoparticles (C) in the region between 1000 and 200 $cm^{-1}$ (a) and in the region between 2500 and 1700 $cm^{-1}$ (b). The inset in panel b shows the Raman spectrum of the hexacyanoferrate(III) ions in the region between 2500 and 1800 $cm^{-1}$.

The Fe−CN vibrational mode is observed at 2131 $cm^{-1}$ in free hexacyanoferrate(III) ions in solution, which is similar to what has been observed in the literature.[26] When the hexacyanoferrate(III) ions are added to the Pt nanoparticles for 2 days, the CN stretching frequency associated with adsorbed hexacyanoferrate(III) ions is observed at 2101 $cm^{-1}$. Adsorbed hexacyanoferrate(III) species have been observed previously[26−35] in Pt, Au, and Ag electrodes and colloids by using SERS, infrared, voltammetry, and other such techniques. The vibrational frequencies associated with the $Pt(CN)_4^{2-}$ complex[36] that we observe are at 2147 and 2167 $cm^{-1}$, which are similar to the literature values[36] of 2149 and 2168 $cm^{-1}$, respectively, that have been reported. In addition, the Pt−C≡N stretching frequency is observed at 2054 $cm^{-1}$, which is similar to that reported in the literature when KCN is exposed to platinum surfaces.[37,38] These bands provide strong evidence that when the platinum nanoparticles are added to hexacyanoferrate(III) ions, the cyanide ions can form a complex with the platinum nanoparticles.

**Raman Studies on the Product Mixture of the Catalyzed and Uncatalyzed Reaction.** We have also conducted Raman studies to determine how the reactants interact with the nanoparticle surface during the electron transfer reaction to form

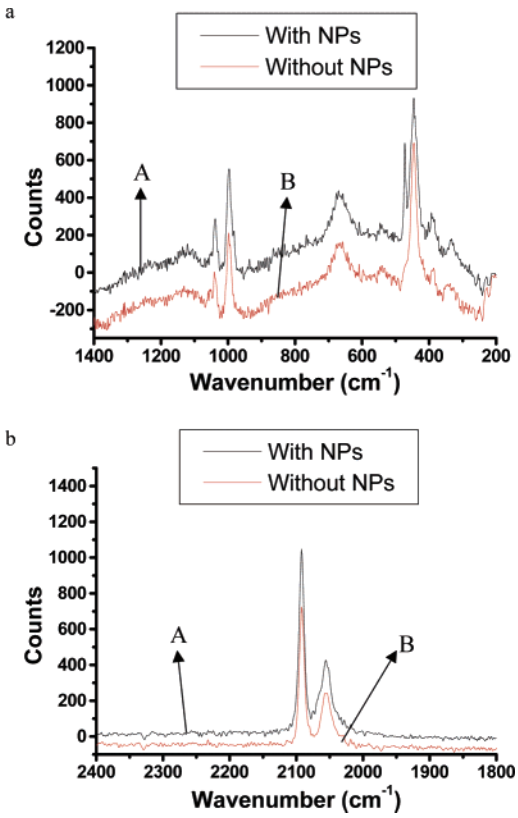


**Figure 3.** Raman spectra of the product mixtures obtained after the electron transfer reaction in the presence of PVP−Pt nanoparticles (A) and in the absence of PVP−Pt nanoparticles (B) in the region from 1400 to 200 $cm^{-1}$ (a) and in the region from 2400 to 1800 $cm^{-1}$ (b).

hexacyanoferrate(II) ions and tetrathionate ions. We have used a 10:1 ratio of thiosulfate to hexacyanoferrate ions to conduct the reaction, and this was done both in the presence and in the absence of the PVP−Pt nanoparticles. The 10:1 ratio was maintained to obtain the Raman spectra of the product mixtures at the actual reaction condition ratio, even though the individual concentrations of the different ions and the nanoparticles are much higher by a factor of 120 for detection of the Raman spectra. To maintain the 10:1 ratio and achieve similar reaction conditions, the thiosulfate concentration is kept at 1 M, the hexacyanoferrate(III) ion concentration is kept at 0.1 M, and the nanoparticle concentration is kept at 17.7 $\mu$M. Figure 3 shows the Raman spectra obtained in the 1400−200 and 2400−1800 $cm^{-1}$ regions. Table 3 summarizes the vibrational frequencies that are important for determining the mechanism of the reaction.

The characteristic vibrational frequencies associated with ferrocyanide[26] (2056 and 2092 $cm^{-1}$) are observed in the product mixture in both cases (with and without the presence of the Pt nanoparticles). It is worth noting that there are no shifts in the characteristic Raman frequencies associated with hexacyanoferrate(II) ions in the product mixture obtained in the presence of the Pt nanoparticles. Also, there is no evidence of frequencies associated with the adsorbed hexacyanoferrate(II) species or frequencies associated with platinum cyanide complexes. Free hexacyanoferrate(III) ions are not left in solution after the reaction since it is the limiting reagent in this reaction.

Since the thiosulfate ions are present in large excess at the beginning of the reaction, there are many free thiosulfate ions left after the reaction is complete. In the product mixture obtained when the reaction is conducted in the presence of the Pt nanoparticles, there is a shift in the symmetric SS stretching

**TABLE 2: List of Characteristic Raman Vibrational Modes Associated with the Hexacyanoferrate(III) Ions and Those Observed upon Exposure to the Pt Nanoparticles as Well as Their Frequencies**

| Raman vibrational mode | hexacyanoferrate(III) ions ($cm^{-1}$) | PVP−Pt nanoparticles + hexacyanoferrate(III) ions ($cm^{-1}$) |
|---|---|---|
| Fe−CN stretching[23] | 389 (s) | − |
| adsorbed Fe−C stretching | − | 368 (w) |
| $(Fe-C)_{br}$ stretching[24,25] | 490 (w) | 487 (m) |
| $(Fe-C)_{rad}$ stretching[24,25] | 540 (w) | 543 (s) |
| $(Fe-C)_{ax}$ stretching[24,25] | 593 (w) | 592 (m) |
| Pt−C≡N stretching[37,38] | − | 2054 (m) |
| adsorbed hexacyanoferrate(III) CN stretching[28] | − | 2101 (s) |
| CN stretching of hexacyanoferrate(III) ions[26] | 2131 (vs) | 2129 (s) |
| surface CN complex with $Pt(CN)_4^{2-}$ species[36] | − | 2147 (m) |
| surface CN Complex with $Pt(CN)_4^{2-}$ species[36] | − | 2167 (m) |

**TABLE 3: List of Characteristic Raman Vibrational Modes and Frequencies after the Electron Transfer Reaction in the Absence of Pt Nanoparticles and in the Presence of Pt Nanoparticles**

| Raman vibrational mode | after the electron transfer reaction (no nanoparticles) ($cm^{-1}$) | after the electron transfer reaction (with Pt nanoparticles) ($cm^{-1}$) |
|---|---|---|
| out-of-plane SSO bending[22] | 338 (w) | 337 (w) |
| symmetric SS stretching[22] | 445 (s) | 446 (s), 473 (m, sh) |
| asymmetric OSO bending[22] | 541 (w) | 542 (w) |
| symmetric OSO bending[22] | 671 (m) | 670 (m) |
| symmetric SO stretching[22] | 998 (s) | 997 (s) |
| asymmetric SO stretching[22] | 1105 (w) | 1105 (w) |
| CN stretching frequency[26] | 2056 (m) | 2056 (m) |
| CN stretching frequency[26] | 2092 (s) | 2092 (s) |

mode that occurs at 473 $cm^{-1}$, suggesting that some of the unreacted thiosulfate ions are bound to the nanoparticle surface. In addition, there are also some free thiosulfate ions present due to the unshifted symmetric SS stretching mode present at 446 $cm^{-1}$. Also, there are no shifts in the other characteristic vibrational frequencies associated with the thiosulfate ions. These observations suggest that during the reaction, the thiosulfate ions bind the nanoparticle surface well, and as a result, the hexacyanoferrate(III) ions preferentially attack the thiosulfate ions rather than the nanoparticle surface to form the hexacyanoferrate(II) ions and tetrathionate ions.

As a result, under the actual reaction conditions, the hexacyanoferrate(III) ions preferentially react with thiosulfate ions rather than with the platinum nanoparticle surface since the thiosulfate ions protect the nanoparticle surface well. Thus, the Raman results support the surface catalytic mechanism for the electron transfer reaction that we proposed previously.[14,17]

## Conclusions

The Raman studies show that the mode of binding of thiosulfate ions involves binding to the platinum nanoparticle surface via the $S^-$ ion. It is also shown that the binding does not take place via the $O^-$ ion since there are no shifts in the symmetric and asymmetric OSO bending or SO stretching vibrations. In addition, it is found that when hexacyanoferrate (III) ions are added to the PVP−Pt nanoparticles, adsorbed hexacyanoferrate(III) species are observed with the adsorbed Fe−C stretching frequency located at 368 $cm^{-1}$ and the adsorbed CN stretching frequency associated with this species located at 2101 $cm^{-1}$. In addition, the $Pt(CN)_4^{2-}$ complex occurs due to the presence of the CN stretching modes at 2147 and 2167 $cm^{-1}$.

In addition, the Pt−C≡N bond forms, and this CN stretching mode occurs at 2054 $cm^{-1}$. This confirms our previous proposal that the hexacyanoferrate(III) ions can attack the nanoparticle surface, resulting in dissolution of surface Pt atoms from the nanoparticles to form a platinum complex with the $CN^-$ ligand present in the hexacyanoferrate(III) ions. The Raman studies on the product mixture obtained after the reaction show that there is no evidence for the formation of adsorbed hexacyanoferrate(II) species as well as no evidence for the formation of any platinum cyanide complexes. In addition, there is evidence for the excess thiosulfate ions binding to the nanoparticle surface after the reaction due to the presence of the shifted symmetric SS stretching frequency. As a result, it can be seen that during the reaction, the thiosulfate ions protect the nanoparticle surface well, and the hexacyanoferrate(III) ions preferentially react with the thiosulfate ions to form products rather than dissolving the nanoparticle surface, confirming the surface catalytic mechanism we proposed previously.

**Acknowledgment.** We thank the NSF Chemistry Division (Grant 0240380) for funding. We also thank Dr. Mohan Srinivasarao for the use of his group's Holoprobe Raman microscope in carrying out the Raman experiments.

## References and Notes

(1) Bradley, J. S. *Clusters Colloids* **1994**, 459.
(2) Duff, D. G.; Baiker, A. *Stud. Surf. Sci. Catal.* **1995**, *91*, 505.
(3) Toshima, N. *NATO ASI Ser., Ser. 3* **1996**, *12*, 371.
(4) Boennermann, H.; Braun, G.; Brijoux, G. B.; Brinkman, R.; Tilling, A. S.; Schulze, S. K.; Siepen, K. *J. Organomet. Chem.* **1996**, *520* (1−2), 143.
(5) Fugami, K. *Organomet. News* **2000**, *1*, 25.
(6) Mayer, A. B. R. *Polym. Adv. Technol.* **2001**, *12* (1−2), 96.
(7) Bonnemann, H.; Richards, R. *Synth. Methods Organomet. Inorg. Chem.* **2002**, *10*, 209.
(8) Moiseev, I. I.; Vargaftik, M. N. *Russ. J. Chem.* **2002**, *72* (4), 512.
(9) Collier, P. J.; Iggo, J. A.; Whyman, R. *J. Mol. Catal. A: Chem.* **1999**, *146* (1−2), 149.
(10) Sculz, J.; Roucoux, A.; Patin, H. *Chem.—Eur. J.* **2000**, *6* (4), 618.
(11) Wang, Q.; Liu, H.; Han, M.; Li, X.; Jiang, D. *J. Mol. Catal. A: Chem.* **1997**, *118* (2), 145.
(12) Kim, S.; Son, S. U.; Lee, S. S.; Hyeon, T.; Chung, Y. K. *Chem. Commun.* **2001**, 2212.
(13) Larpent, C.; Menn, B. F.; Patin, H. *J. Mol. Catal.* **1991**, *65*, L35.
(14) Narayanan, R.; El-Sayed, M. A. *J. Phys. Chem. B* **2003**, *107* (45), 12416.
(15) Narayanan, R.; El-Sayed, M. A. *Nano Lett.* **2004**, *4* (7), 1353.
(16) Narayanan, R.; El-Sayed, M. A. *J. Am. Chem. Soc.* **2004**, *126* (23), 7419.
(17) Narayanan, R.; El-Sayed, M. A. *J. Phys. Chem. B* **2004**, *108* (18), 5726.
(18) Narayanan, R.; El-Sayed, M. A. *J. Am. Chem. Soc.* **2003**, *125* (27), 8340.
(19) Narayanan, R.; El-Sayed, M. A. *J. Phys. Chem. B* **2004**, *108* (25), 8572.
(20) Narayanan, R.; El-Sayed, M. A. *Langmuir* **2005**, *21* (5), 2027.
(21) Narayanan, R.; El-Sayed, M. A. *J. Phys. Chem. B* **2005**, *109* (10), 4357.
(22) Rintoul, L.; Crawford, K.; Shurvell, H. F.; Fredericks, P. M. *Vib. Spectrosc.* **1997**, *15*, 171.
(23) Griffith, W. P.; Turner, G. T. *J. Chem. Soc. A* **1970**, 858.
(24) Pfennig, B. W.; Lockard, J. V.; Cohen, J. L.; Watson, D. F.; Ho, D. M.; Bocarsly, A. B. *Inorg. Chem.* **1999**, *38*, 2941.
(25) Nakamoto, K. *Infrared and Raman Spectra of Inorganic and Coordination Compounds*, 4th ed.; John Wiley & Sons: New York, 1986.
(26) Loo, B. H.; Lee, Y. G.; Liang, E. J.; Kiefer, W. *Chem. Phys. Lett.* **1998**, *297*, 83.
(27) Loo, B. H. *Chem. Phys. Lett.* **1993**, *213* (5−6), 479.
(28) Lowry, R. B. *J. Raman Spectrosc.* **1991**, *22*, 805.
(29) Wieckowski, A.; Szklarczyk, M. *J. Electroanal. Chem.* **1982**, *142*, 157.
(30) Kunimatsu, K.; Shigematsu, Y.; Uosaki, K.; Kita, H. *J. Electroanal. Chem.* **1989**, *262*, 195.
(31) Pons, S.; Datta, M.; McAleer, J. F.; Hinman, A. S. *J. Electroanal. Chem.* **1984**, *160*, 369.
(32) Fleischmann, M.; Graves, P. R.; Robinson, J. *J. Electroanal. Chem.* **1985**, *182*, 87.
(33) Lowry, R. B. *Spectrochim. Acta* **1993**, *49A*, 831.
(34) Huang, W.; McCreery, R. *J. Electroanal. Chem.* **1992**, *326*, 1.
(35) Niwa, K.; Doblhofer, K. *Electrochim. Acta* **1986**, *31* (4), 439.
(36) Kubas, G. J.; Jones, L. H. *Inorg. Chem.* **1974**, *13* (12), 2816.
(37) Ren, B.; Li, X. Q.; Wu, D. Y.; Yao, J. L.; Xie, Y.; Tian, Z. Q. *Chem. Phys. Lett.* **2000**, *322*, 561.
(38) Ren, B.; Wu, D.-Y.; Mao, B.-W., Tian, Z.-Q. *J. Phys. Chem. B* **2003**, *107* (12), 2752.